Supporting Information

Near-Infrared Chemiluminescent Probe for Real-Time Monitoring of Nitroreductase in Tumors

Pan Zhu,[a,†] Yu Tang,[b,†] Yuanyu Tang,[a] Shaojing Zhao,[a,] Fei Long,[c] Chaoyi Yao,[a] Benhua Wang,[a] Xiangzhi Song,[a] Yi Zhang,[c,*] Chaochao Tan[d,*] and Minhuan Lan[a,*]*

[a]College of Chemistry and Chemical Engineering, Central South University, Changsha, 410083, P. R. China. E-mails: 31180030@csu.edu.cn; minhuanlan@csu.edu.cn

[b]Gastroenterology and Urology Department Ⅱ, The Affiliated Cancer Hospital of Xiangya School of Medicine, Central South University/Hunan Cancer Hospital, Changsha, 410013, P. R. China.

[c]Department of Gastrointestinal Surgery, The Third Xiangya Hospital of Central South University, Changsha, 410013, P. R. China. E-mail: yzhangxy3@csu.edu.cn

[d]Department of Clinical Laboratory, The First Affiliated Hospital of Hunan Normal University (Hunan Provincial People's Hospital), Changsha, 410005, P. R. China. E-mail: tchchwolf@163.com

[†] P. Z. and Y. T. contributed to this work equally.

1. Experimental General

Instruments and materials. Unless otherwise stated, all solvents and chemicals were purchased from commercial suppliers in analytical grade and used without further purification. Ultrapure water was used in all spectroscopic studies. The ^{1}H and ^{13}C NMR spectra were recorded on a Bruker AVANCE III 400 or 500 spectrometer, using TMS as an internal standard. The high-resolution mass spectrometry data was obtained from the Bruker compact instrument. Absorption spectra were collected on a Shimadzu UV-2600 spectrophotometer, and fluorescence spectra were performed on a Shimadzu RF-6000 spectrophotometer.

Spectral test. Ad-TCN-CL dissolved in PBS (pH = 7.4, containing 10% DMSO). Then, the absorption and fluorescence spectra (λ_{ex} = 550 nm) of the solution were acquired by UV-2600 and RF-6000 spectrometers, respectively. For the chemiluminescence spectrum, **Ad-TCN-CL** in PBS was placed in a black 96-well plate, followed by imaging using PerkinElmer IVIS instrument. Finally, the quantification of images was conducted by region of interesting (ROI) analysis using Living Imaging software, and the chemiluminescence spectrum was plotting (chemiluminescence imaging parameters: bioluminescence mode, emission channel: 520, 570, 620, 670, 710, and 790 nm, Auto for exposure, field of view: D).

Tissue penetration assay. Ad-TCN-CL or **Ad-TCN** in PBS (100 μM) was placed in a black 96-well plate, and then covered with chicken tissues of different thicknesses (2, 5, 8, and 10 mm). Subsequently, the chemiluminescence and fluorescence imaging were carried out respectively by IVIS instrument.

Chemiluminescence kinetics: 600 μL **NTR-TCN-CL** solution (25 μM), containing NADH (500 μM), was incubated with NTRase (10 μg/mL) at different moments at 37 °C. After that, the chemiluminescence images of **NTR-TCN-CL** at different moments were acquired simultaneously by IVIS instrument.

Chemiluminescence assays *in vitro*. For imaging of **NTR-TCN-CL** of different concentrations, 2 μM NADH (50 mM) and NTRase (1 mg/mL) dissolved in PBS. After that, to the above mixture were added **NTR-TCN-CL** solution (1 mM) of varying volumes (1.5, 3, 5, 7.5, 10 μL), making the total volume of the solution 200 μL. Imaging was performed 10 min after incubation at 37 °C. For imaging of **NTR-TCN-CL** with NTRase of different concentrations, NTRase (0.1 mg/mL or 1 mg/mL) of different volumes (1.0, 2.0, 3.0, 4.0 μL or 0.5, 1.0, 1.5, 2.0, 4.0, 6.0, 8.0 μL) were added into the PBS containing 25 μM **NTR-TCN-CL** and 500 μM NADH respectively, followed by imaging after incubation at 37 °C for 10 min. The LOD was calculated based on the standard deviation of the blank signal (σ) and the slope of the calibration curve (S), using the universally accepted formula: LOD = 3σ/S.

Hemolysis Assay *in vitro*. The specific experimental process was as follows, mouse red blood

cell suspension was added to different materials (**NTR-TCN-CL** and **TCN-OMe**) at a concentration of 100 μM at 37 ℃. After 3 h, the supernatant of erythrocyte suspension was collected by centrifugation, and measured by the Thermo Fisher microplate reader at 540 nm. PBS and H_2O were performed as the negative group and the positive group, respectively. The hemolysis rate was calculated according to the formula below:

$$Hemolysis\ rate = \frac{A_{T540} - A_{B540} - A_{N540}}{A_{P540} - A_{N540}} \times 100\%$$

Where A_{T540}, A_{N540}, and A_{P540} represent the absorbance values of the supernatant for the test group (**NTR-TCN-CL** or **TCN-OMe**), the negative group, and the positive group, respectively, and A_{B540} denotes the absorbance value for the **NTR-TCN-CL** or **TCN-OMe** disolved in PBS.

Chemiluminescence assays *in vivo*. For imaging of exogenous NTRase, firstly, NTRase (20 μg/mL) + NADH (500 μM) and PBS were injected into the left and right dorsa of a healthy mouse respectively. Secondly, the mouse's left and right dorsa were administrated with 200 μL **NTR-TCN-CL** (100 μM), followed by imaging. As for as imaging of endogenous NTRase, the 4T1 tumor-bearing mice were divided into two groups "PBS" and "$CoCl_2$". Namely, the mouse was treated with PBS or $CoCl_2$ (200 μM), respectively. After 2 h, them were administrated with **NTR-TCN-CL**, and imaging was performed immediately.

All animal procedures were performed in accordance with the Guidelines for Care and Use of Laboratory Animals of Hunan Normal University (China) and approved by the Animal Ethics Committee of Hunan Normal University (No. D2024026).

2. Theoretical Calculation Details

The theoretical calculations were performed via the Gaussian 16, Revision C.01[1]. The geometries of protonated and deprotonated **TCN-OMe** were optimized using PEB0 functional with def2-TZVP basis set with SMD solvent model to describe the water environment. Their highest occupied molecular orbital (HOMO) and the lowest unoccupied molecular orbital (LUMO) were analyzed based on the optimized structures in the ground state.

3. Synthetic Methods.

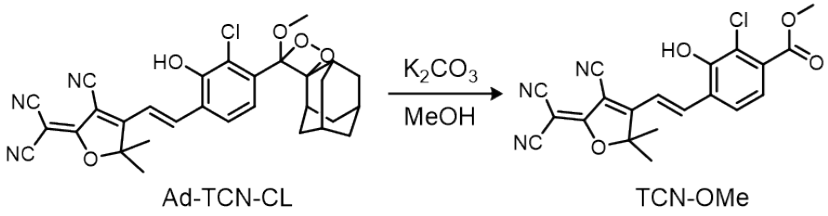

Scheme S1. Synthesis route of **TCN-OMe**.

P-Ad and **TCN** were synthesized according to the literatures[2,3].

P-Ad (yield: 60%, off-white solid)**:** ^{1}H NMR (400 MHz, Chloroform-d) δ 11.62 (s, 1H), 9.90 (s, 1H), 7.49 (d, J = 7.8 Hz, 1H), 6.99 (d, J = 7.8 Hz, 1H), 3.34 (s, 3H), 3.28 (s, 1H), 2.08 (s, 1H), 1.98 - 1.74 (m, 12H). ^{13}C NMR (101 MHz, Chloroform-d) δ 195.69, 130.89, 122.89, 76.70, 57.53, 39.24, 39.05, 38.59, 38.48, 37.00, 32.98, 29.76, 28.32, 28.16.

TCN (yield: 52%, white solid)**:** ^{1}H NMR (400 MHz, DMSO-d_6) δ 2.37 (s, 3H), 1.60 (s, 6H). ^{13}C NMR (101 MHz, DMSO-d6) δ 186.23, 177.75, 112.69, 111.97, 110.44, 104.12, 101.81, 55.26, 40.65, 23.70, 14.67.

Synthesis of Ad-TCN

P-Ad (100 mg, 0.3 mmol) and **TCN** (72 mg, 0.36 mmol) were dissolved in 5 ml of acetonitrile (ACN). To the above mixture was added piperidine (Pip.) (60 μL, 0.6 mmol). The reaction solution was refluxed under nitrogen atmosphere, and the progress of the reaction was monitored by TLC. Upon completion, the reaction solution was diluted with dichloromethane (DCM), neutralized with diluted hydrochloric acid and washed with water. The organic phase was dried with anhydrous sodium sulfate. The crude product was purified by silica gel column chromatography (petroleum ether (PE)/DCM = 1/20) to obtain orange solid (40 mg, yield: 26%). ^{1}H NMR (400 MHz, Chloroform-d) δ 7.94 (d, J = 16.6 Hz, 1H), 7.54 (d, J = 8.1 Hz, 1H), 7.22 (s, 1H), 6.97 (d, J = 8.1 Hz, 1H), 3.33 (s, 3H), 3.28 (s, 1H), 2.12 (s, 1H), 2.01 - 1.84 (m, 8H), 1.82 (s, 6H), 1.76 (s, 4H). ^{13}C NMR (101 MHz, Chloroform-d) δ 175.16, 174.16, 151.45, 141.19, 139.38, 139.02, 134.26, 126.34, 124.37, 121.92, 121.35, 116.31, 111.56, 110.79, 110.03, 100.47, 97.72, 57.59, 36.93, 33.07, 31.93, 31.51, 30.14, 29.82, 29.70, 28.18, 26.62. HRMS (ESI) m/z: $[M + Na]^+$ calcd. for $C_{30}H_{28}ClN_3O_3$, 536.1711; found. 536.1741.

Synthesis of Ad-TCN-CL

Ad-TCN (15 mg, 0.03 mmol) (scheme S1) and methylene blue (MB) (1 mg, 0.003 mmol) were dissolved in 10 mL of DCM. The mixture above was then allowed to cool to 0 °C and oxygen was bubbled through the solution while irradiating with yellow light (50 W/cm^2). The reaction progress was monitored by TLC. Upon completion, **Ad-TCN-CL** was obtained by silica gel column

chromatography with DCM as the eluent (11 mg, yield: 68%). ^{1}H NMR (400 MHz, Chloroform-*d*) δ 7.95 (d, *J* = 16.6 Hz, 1H), 7.85 - 7.74 (m, 1H), 7.66 (d, *J* = 8.4 Hz, 1H), 7.31 (s, 1H), 3.24 (s, 3H), 3.03 (s, 1H), 2.20 (s, 1H), 2.02 (s, 1H), 1.83 (s, 6H), 1.79 - 1.41 (m, 11H). ^{13}C NMR (101 MHz, Chloroform-*d*) δ 175.02, 173.89, 140.68, 136.51, 126.59, 125.23, 117.55, 111.38, 110.67, 109.91, 101.16, 97.84, 97.81, 96.41, 50.87, 49.75, 36.46, 34.09, 33.56, 32.96, 32.13, 31.62, 31.56, 29.68, 26.53, 26.09, 25.78. HRMS (ESI) m/z: $[M + K]^+$ calcd. for $C_{30}H_{28}ClN_3O_5$, 584.1349; found, 584.1320.

Synthesis of TCN-OMe

Ad-TCN-CL (11 mg, 0.02 mmol) was dissolved in 2 mL of methanol followed by addition of 5 mg of K_2CO_3. After completion, the solvent was removed under reduced pressure. The crude product was purified by silica gel column chromatography with DCM as the eluent to afford **TCN-OMe** as an orange solid (6 mg, yield 75 %). ^{1}H NMR (400 MHz, DMSO-d_6) δ 8.22 (d, *J* = 16.6 Hz, 1H), 7.98 (d, *J* = 8.3 Hz, 1H), 7.43 (d, *J* = 16.5 Hz, 1H), 7.34 (d, *J* = 8.3 Hz, 1H), 3.87 (s, 3H), 1.77 (s, 6H).

Synthesis of P-Ad-NTR

P-Ad (100 mg, 0.3 mmol) was dissolved in 10 mL of acetonitrile and potassium carbonate (70 mg, 0.5 mmol) was added immediately. After stirring for 10 min at room temperature, *p*-nitrobenzyl bromide (77 mg, 0.36 mmol) was added to the above mixture, and the reaction solution was stirred at room temperature. At the end of the reaction, the solid in the reaction solution was filtered off and the crude product was purified using silica gel column chromatography (PE/ethyl acetate = 10/1) to obtain a light-yellow solid **P-Ad-NTR** (120 mg, yield: 78%). ^{1}H NMR (400 MHz, Chloroform-d) δ 10.28 (s, 1H), 8.29 (d, J = 8.7 Hz, 2H), 7.77 (d, J = 7.9 Hz, 1H), 7.70 (d, J = 8.5 Hz, 2H), 7.24 (d, J = 7.9 Hz, 1H), 5.26 (d, J = 10.5 Hz, 2H), 3.35 (s, 3H), 3.29 (s, 1H), 2.07 (s, 1H), 1.98 – 1.76 (m, 12H). ^{13}C NMR (100 MHz, Chloroform-d) δ 188.40, 157.03, 147.98, 143.04, 142.91, 138.99, 133.89, 130.14, 129.64, 128.45, 126.77, 123.91, 75.64, 57.65, 39.27, 39.17, 39.04, 38.69, 38.58, 36.94, 33.03, 29.77, 28.27, 28.12. HRMS (ESI) m/z: $[M + Na]^+$ calcd. for $C_{26}H_{26}ClNO_5$, 506.1705; found, 506.1244.

Synthesis of NTR-TCN

TCN (40 mg, 0.2 mmol) and **P-Ad-NTR** (110 mg, 0.24 mmol) were first dissolved in 5 mL of ACN, followed by the addition of Pip. (50 μL, 0.5 mmol). The reaction solution was refluxed under nitrogen atmosphere. At the end of the reaction, the organic phase was diluted with DCM, washed with diluted hydrochloric acid and water, and finally dried with anhydrous sodium sulfate. The crude product was purified by silica gel column chromatography (DCM/PE = 5/1) to obtain a yellow solid (20 mg, yield: 15%). ^{1}H NMR (400 MHz, Chloroform-d) δ 8.29 (d, J = 8.7 Hz, 2H), 8.01 (d,

J = 16.6 Hz, 1H), 7.71 (d, J = 8.7 Hz, 2H), 7.65 (d, J = 8.1 Hz, 1H), 7.24 (d, J = 8.1 Hz, 1H), 7.01 (d, J = 16.6 Hz, 1H), 5.20 (d, J = 7.5 Hz, 2H), 3.36 (s, 3H), 3.30 (s, 1H), 2.08 (s, 1H), 1.99 – 1.63 (m, 12H), 1.63 (s, 6H). ^{13}C NMR (100 MHz, Chloroform-d) δ 174.82, 173.19, 154.47, 148.11, 142.82, 141.25, 140.33, 138.97, 134.24, 129.98, 128.73, 128.40, 124.98, 124.37, 123.97, 123.47, 116.48, 111.22, 110.52, 110.15, 100.75, 97.57, 74.92, 57.64, 36.94, 34.98, 34.44, 33.19, 31.51, 31.44, 30.15, 29.86, 29.69, 28.24, 26.08. HRMS (ESI) m/z: $[M + Na]^+$ calcd. for $C_{37}H_{33}ClN_4O_5$; 671.2032; found, 671.2037.

The synthetic details for **NTR-TCN-CL** are the same as that for **Ad-TCN-CL**.

NTR-TCN-CL: 65% yield. ^{1}H NMR (400 MHz, Chloroform-*d*) δ 8.29 (d, J = 8.7 Hz, 2H), 8.11 – 8.01 (m, 2H), 7.74 (dd, J = 19.8, 8.5 Hz, 3H), 7.04 (d, J = 16.6 Hz, 1H), 5.11 (s, 2H), 3.25 (s, 3H), 3.03 (s, 1H), 2.27 (d, J = 10.1 Hz, 1H), 2.04 – 1.58 (m, 18H). ^{13}C NMR (126 MHz, Chloroform-*d*) δ 148.12, 142.52, 139.64, 138.12, 130.57, 129.89, 128.32, 125.09, 124.01, 117.57, 111.49, 111.12, 110.42, 110.13, 97.74, 96.48, 74.98, 49.83, 36.48, 33.89, 33.73, 32.16, 31.55, 31.44, 29.70, 26.08, 25.96, 25.79. HRMS (ESI) m/z: $[M + K]^+$ calcd. for $C_{37}H_{33}ClN_4O_7$, 719.1670; found, 719.1844.

4. Supplementary Figures

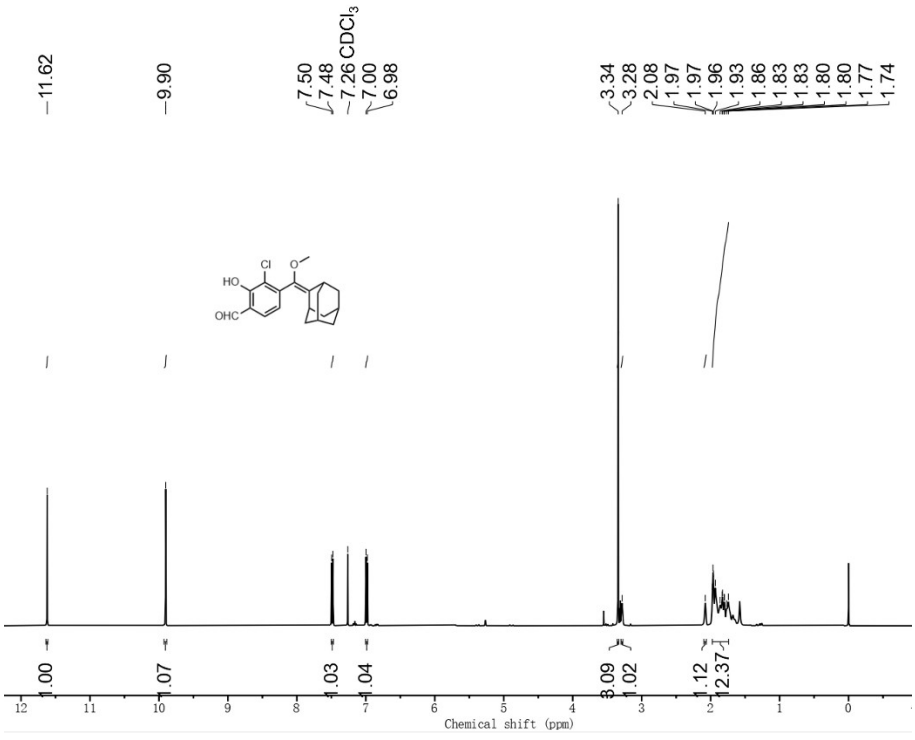

Fig. S1 ^{1}H NMR spectrum of **P-Ad** in $CDCl_3$.

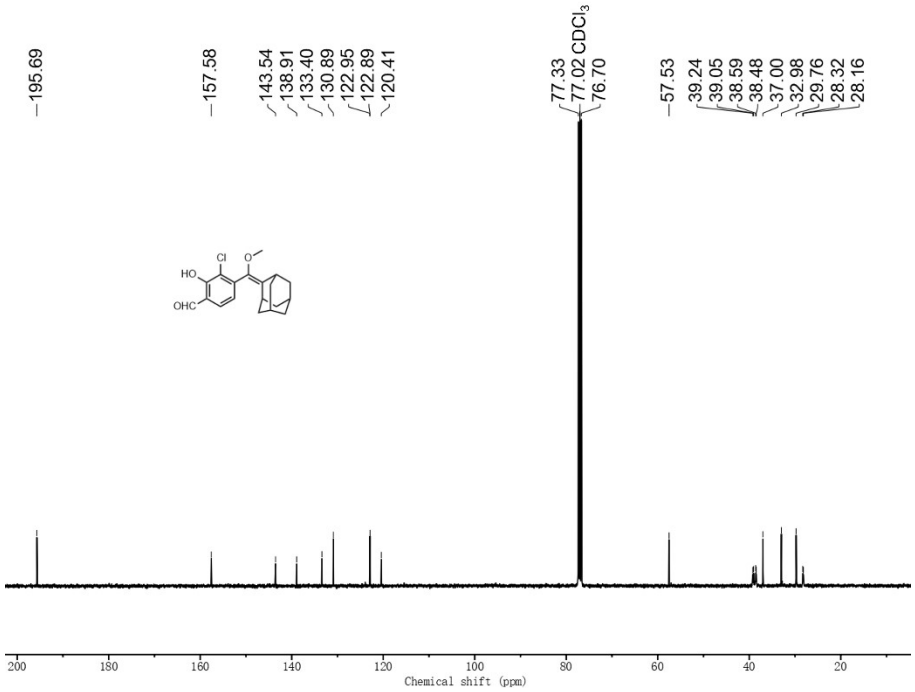

Fig. S2 ^{13}C NMR spectrum of **P-Ad** in $CDCl_3$.

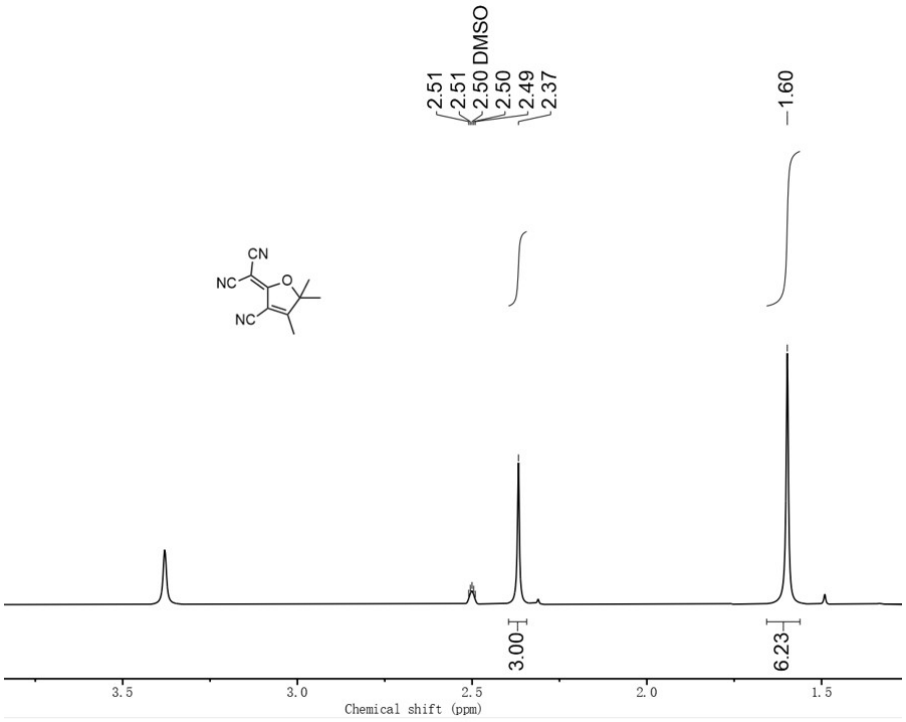

Fig. S3 ^{1}H NMR spectrum of **TCN** in DMSO-d_6.

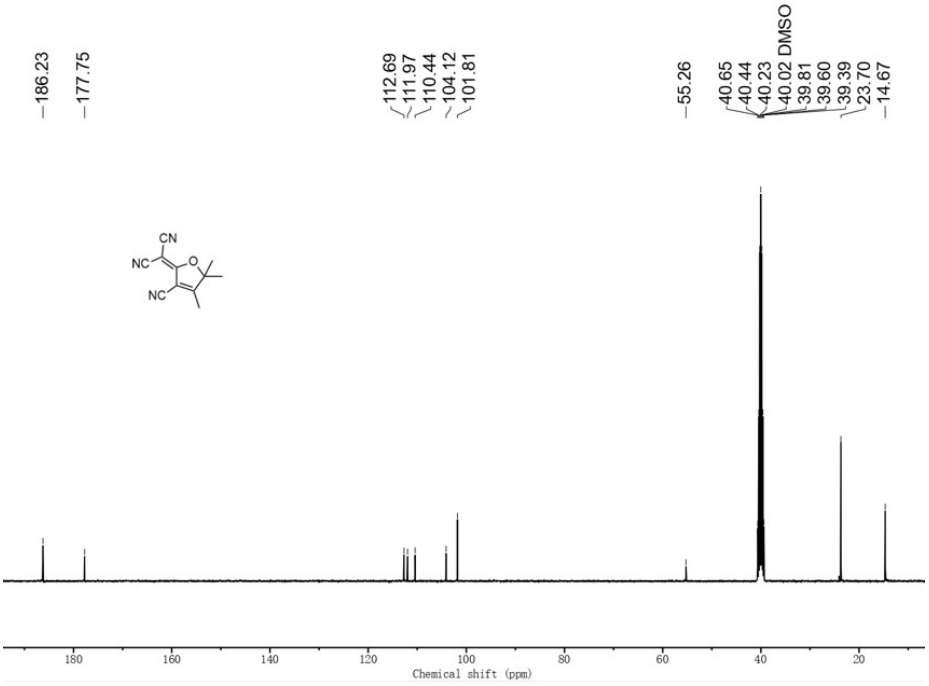

Fig. S4 ^{13}C NMR spectrum of **TCN** in DMSO-d_6.

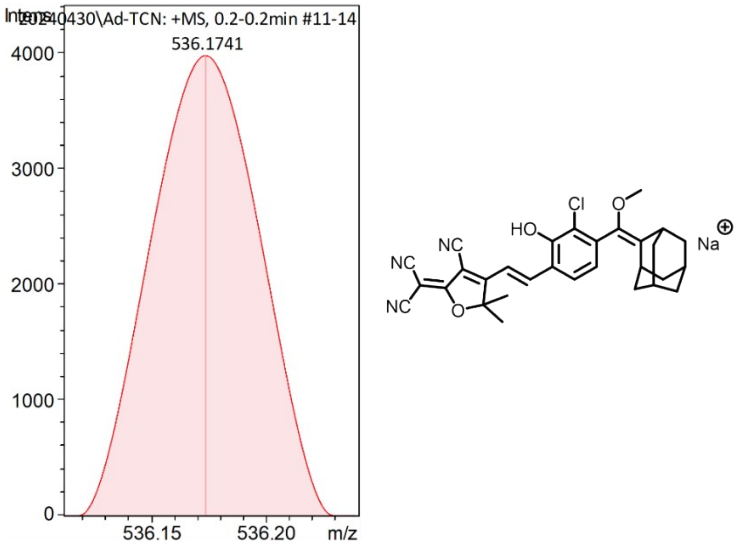

Fig. S5 HRMS spectrum of **Ad-TCN** + Na^+.

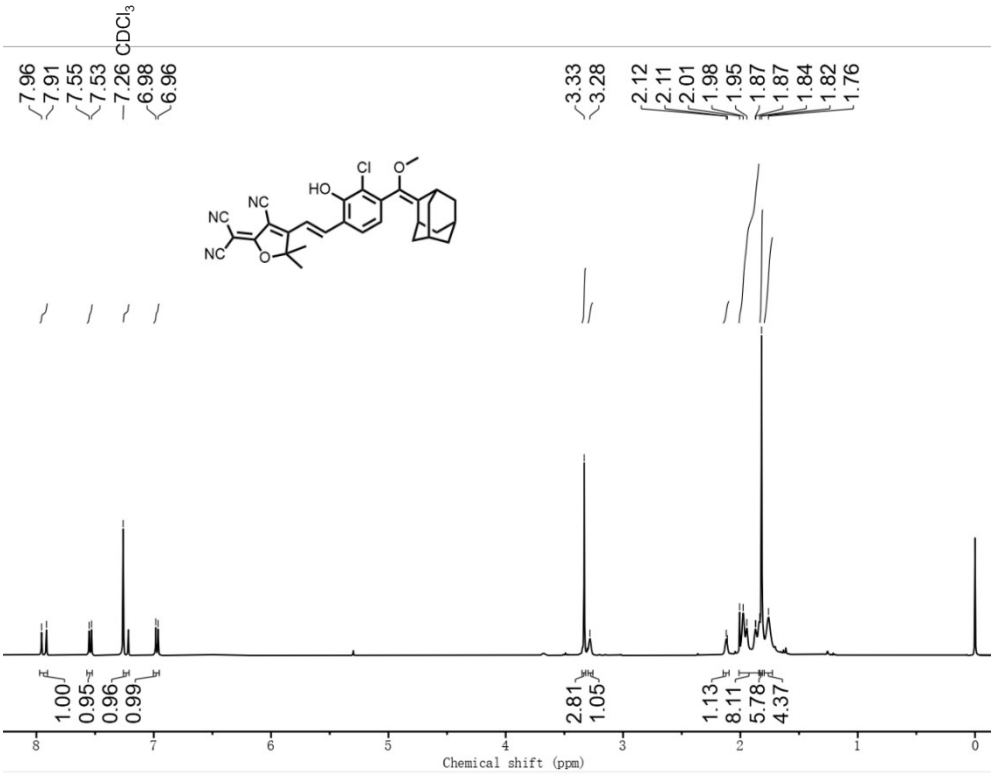

Fig. S6 ^{1}H NMR spectrum of **Ad-TCN** in $CDCl_3$.

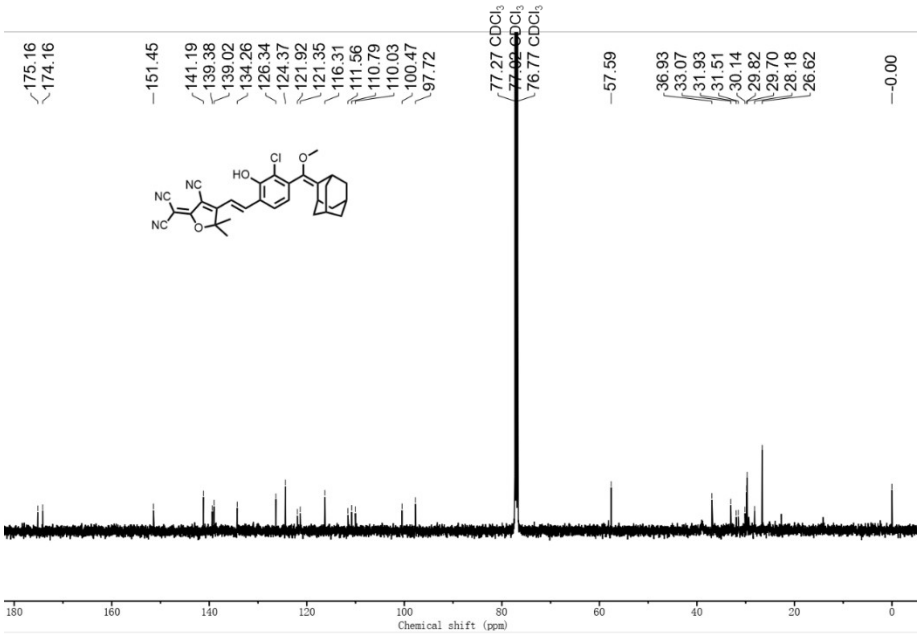

Fig. S7 ^{13}C NMR spectrum of **Ad-TCN** in $CDCl_3$.

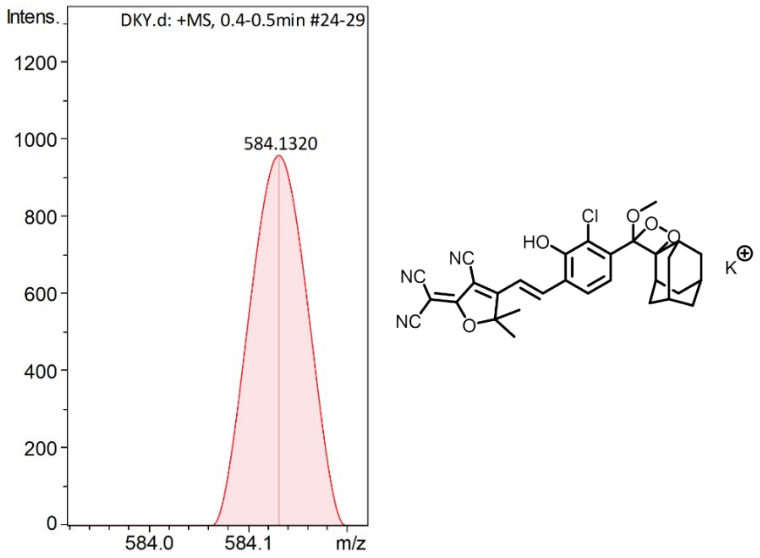

Fig. S8 HRMS spectrum of **Ad-TCN-CL** + K^+.

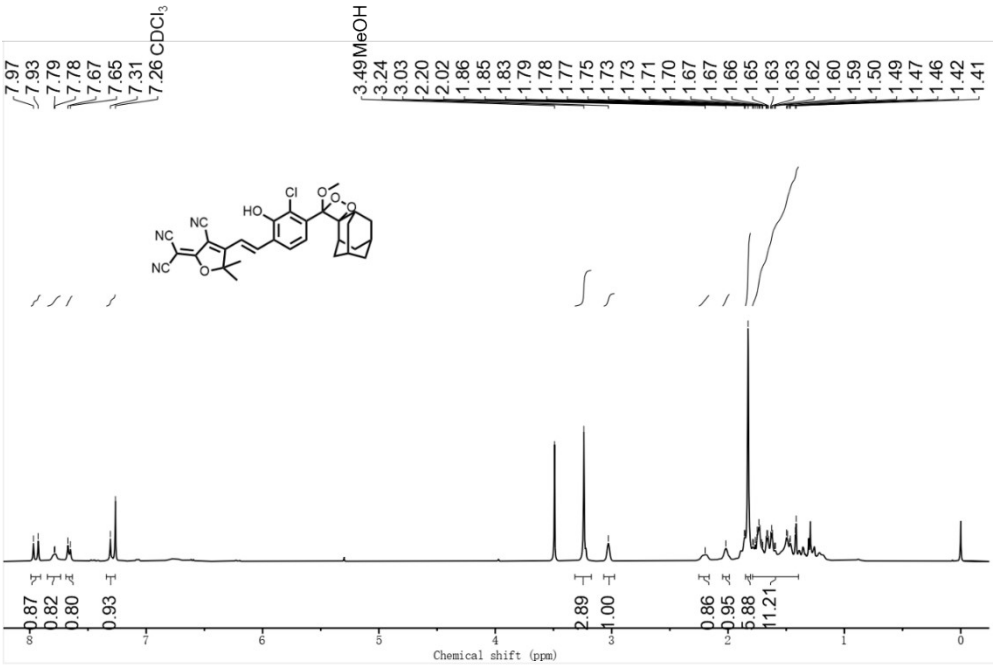

Fig. S9 ^{1}H NMR spectrum of **Ad-TCN-CL** in $CDCl_3$.

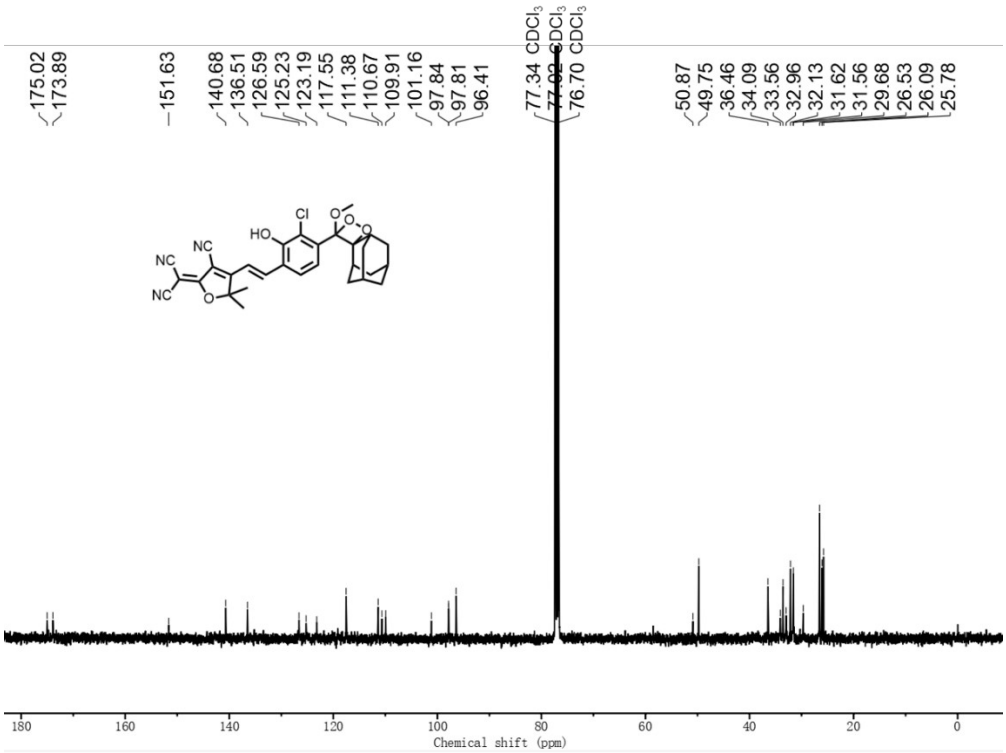

Fig. S10 ^{13}C NMR spectrum of **Ad-TCN-CL** in $CDCl_3$.

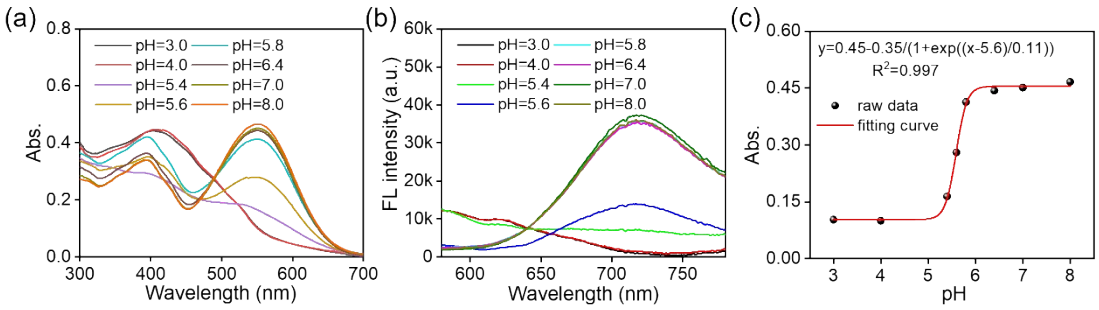

Fig. S11 (a) Absorption and (d) fluorescence spectra (λ_{ex} = 550 nm) of **TCN-OMe** in PBS buffer of different pH values. (c) Non-linear relationship between the absorbance at 550 nm and the pH values.

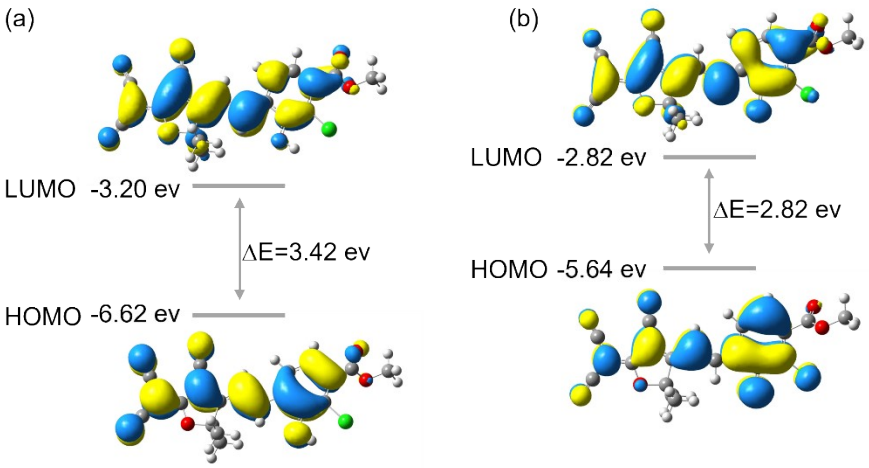

Fig. S12 The LUMO, HOMO distributions and their energy gap of (a) protonated **TCN-OMe** and (b) deprotonated **TCN-OMe** at the minimum energy states of the electronic ground state.

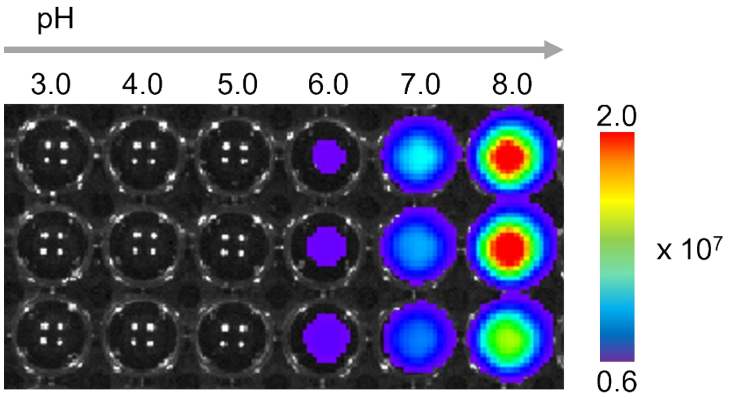

Fig. S13 Chemiluminescence images of **Ad-TCN-CL** (100 μM) in PBS with different pH values.

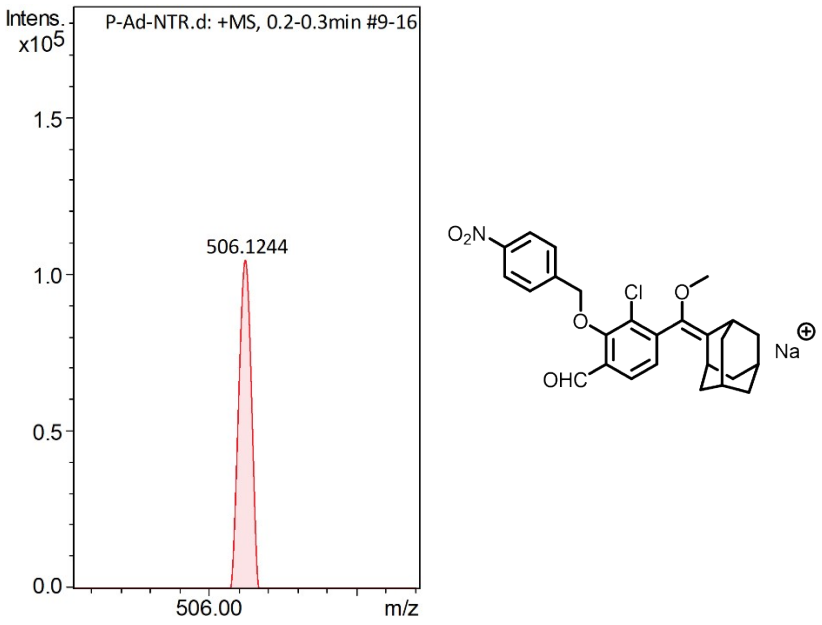

Fig. S14 HRMS spectrum of **P-Ad-TCN** + Na^+.

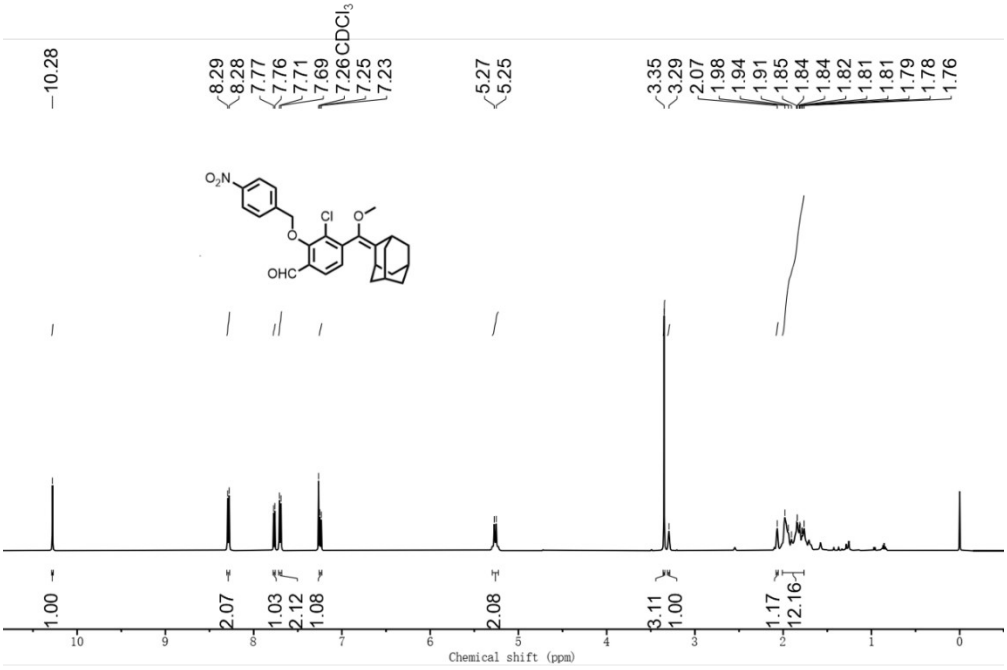

Fig. S15 ^1H NMR spectrum of **P-Ad-TCN** in $CDCl_3$.

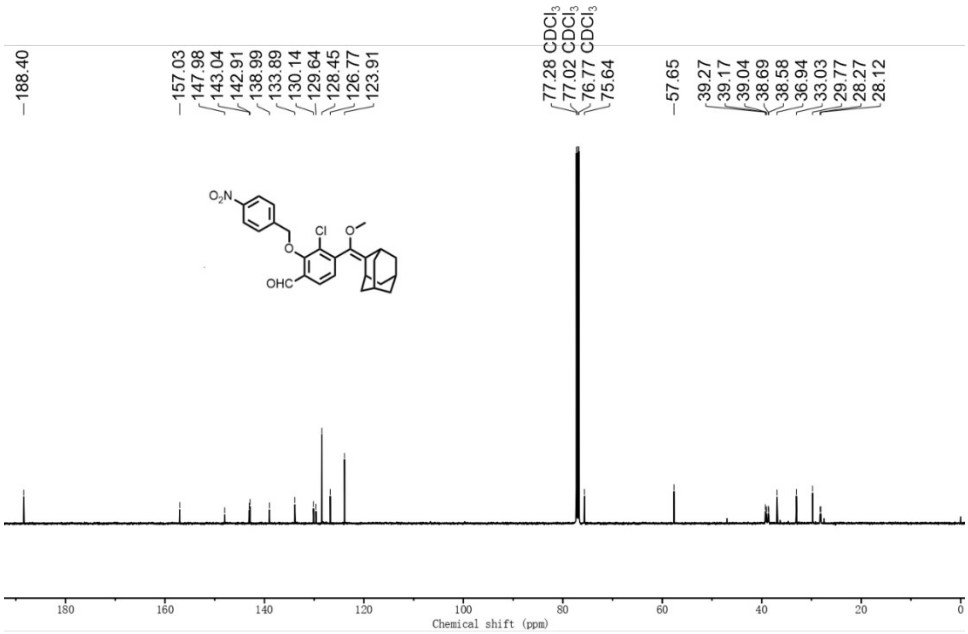

Fig. S16 ^{13}C NMR spectrum of **P-Ad-TCN** in $CDCl_3$.

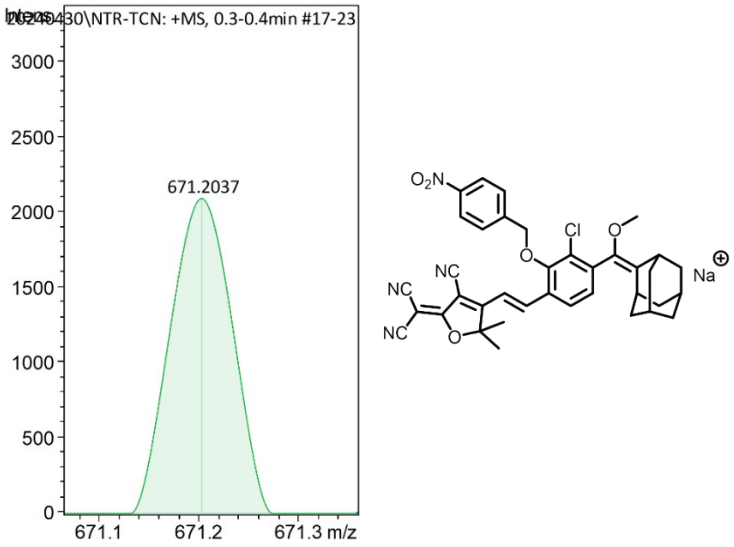

Fig. S17 HRMS spectrum of **NTR-TCN** + Na^+.

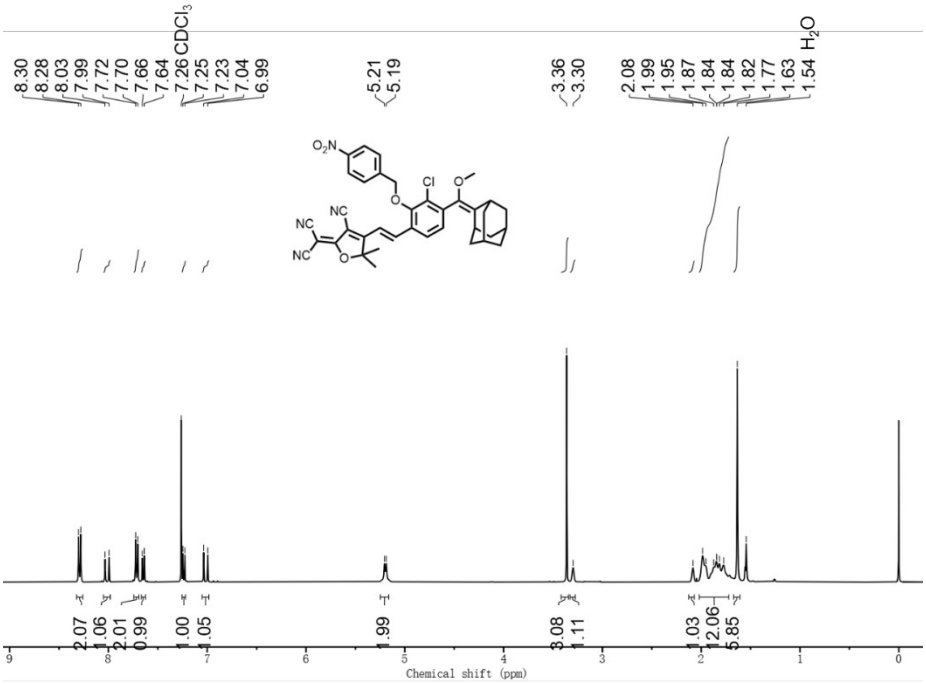

Fig. S18 ^{1}H NMR spectrum of **NTR-TCN** in $CDCl_3$.

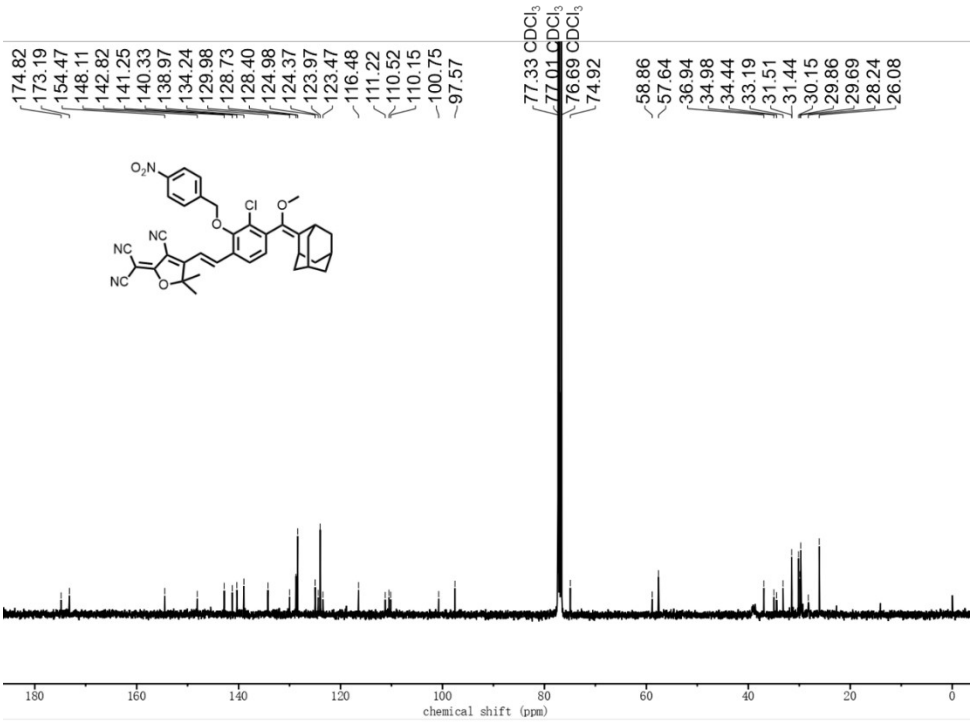

Fig. S19 ^{13}C NMR spectrum of **NTR-TCN** in $CDCl_3$.

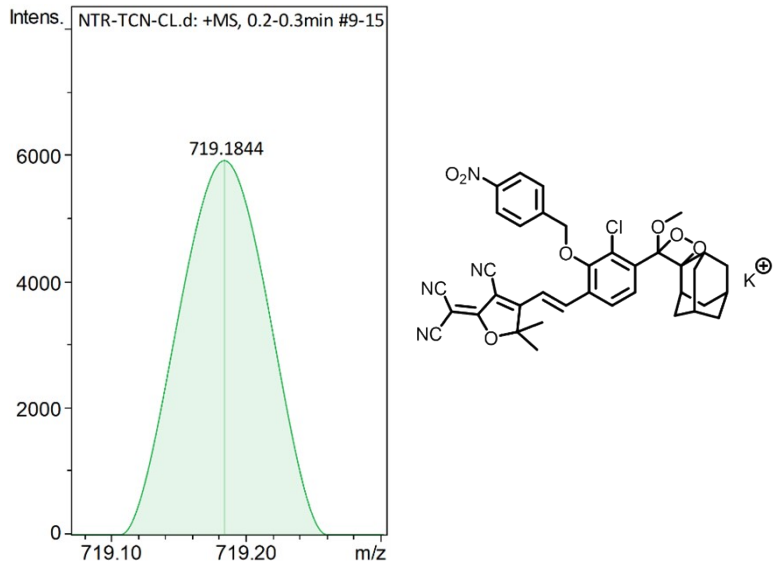

Fig. S20 HRMS spectrum of **NTR-TCN-CL** + K^+.

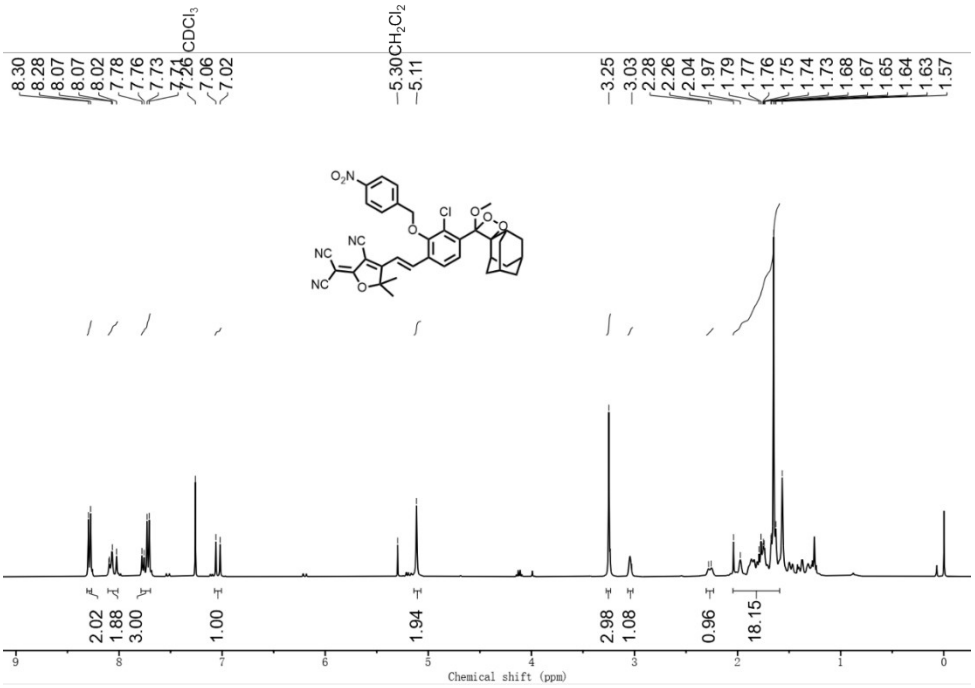

Fig. S21 ^{1}H NMR spectrum of **NTR-TCN-CL** in $CDCl_3$.

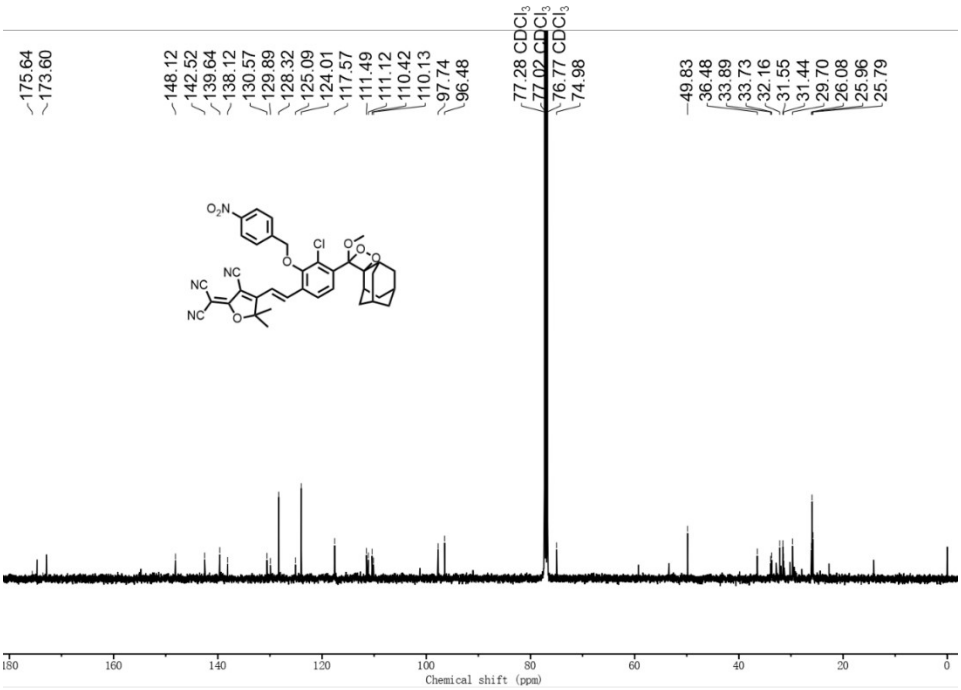

Fig. S22 ^{13}C NMR spectrum of **NTR-TCN-CL** in $CDCl_3$.

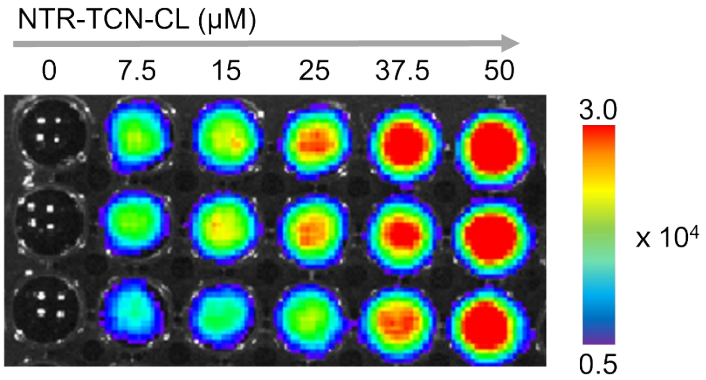

Fig. S23 Chemiluminescence images of different concentration of **NTR-TCN-CL**.

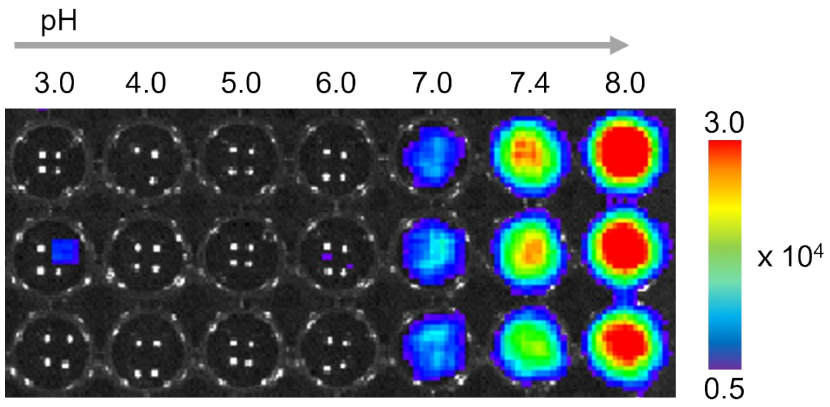

Fig. S24 Chemiluminescence images of **NTR-TCN-CL** (25 μM) in PBS with different pH values in the presence of NTRase (10 μg/mL).

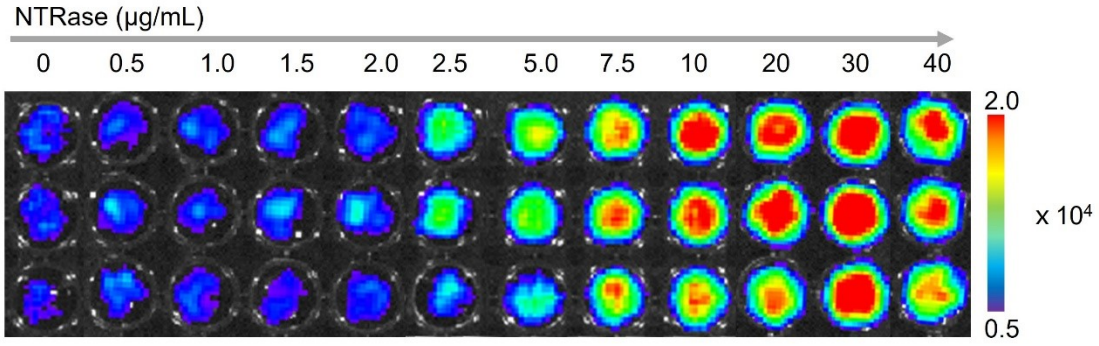

Fig. S25 Chemiluminescence images of **NTR-TCN-CL** (25 μM) treated with different concentration of NTRase.

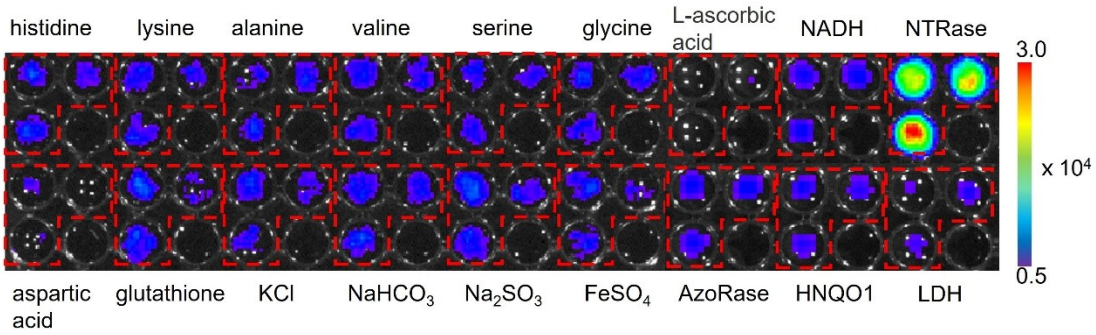

Fig. S26 Chemiluminescence images of **NTR-TCN-CL** (25 μM) treated with various analysts (AzoRase, HNQO1, LDH, and NTRase: 10 μg/mL, others: 500 μM).

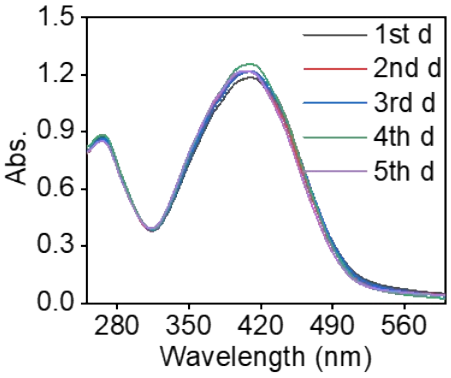

Fig. S27 Absorption spectra of **NTR-TCN-CL** stored at 4 ºC within 5 days.

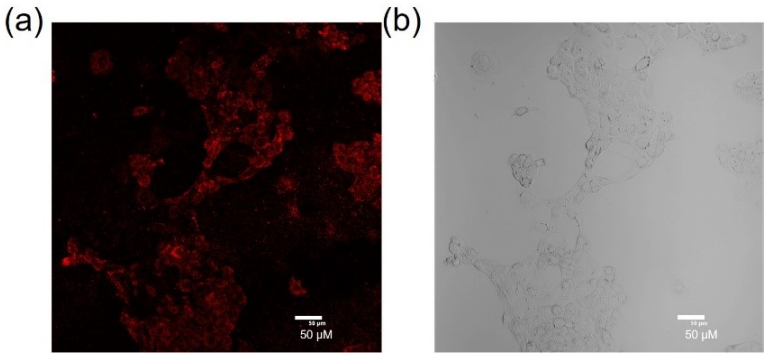

Fig. S28 (a) Fluorescence image and (b) photograph of 4T1 cells incubated with **NTR-TCN-CL** for 15 min.

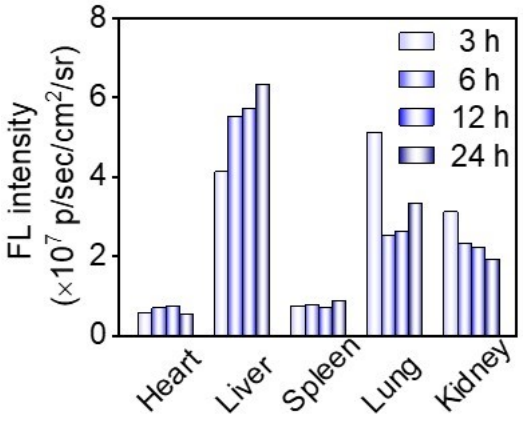

Fig. S29 Fluorescence intensities of ex vivo organs at 3, 6, 12 and 24 h after tail vein injection of

NTR-TCN-CL (100 μM).

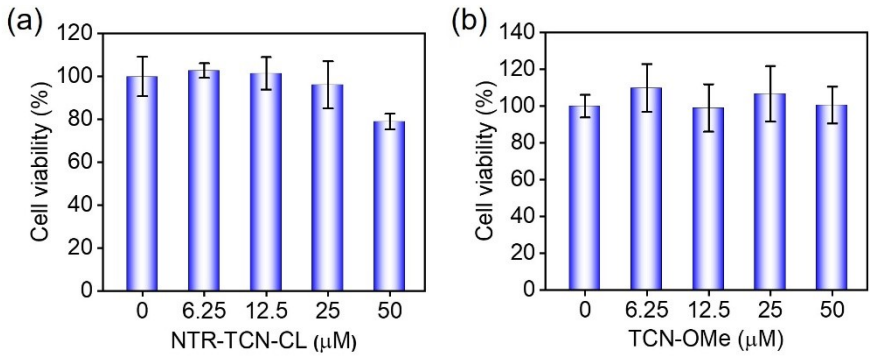

Fig. S30 Chemical toxicity of **NTR-TCN-CL** and (b) **TCN-OMe** at different concentrations to 4T1 cells.

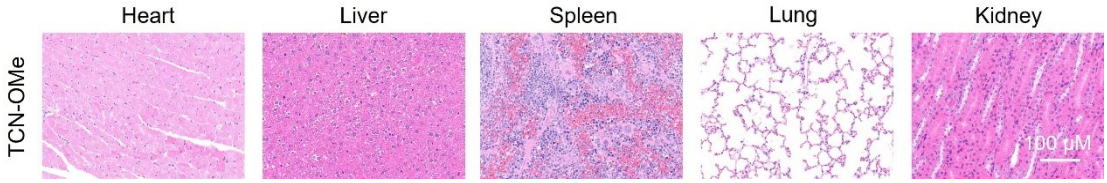

Fig. S31 H&E staining of major organs of the mice after treatment of **TCN-OMe**.

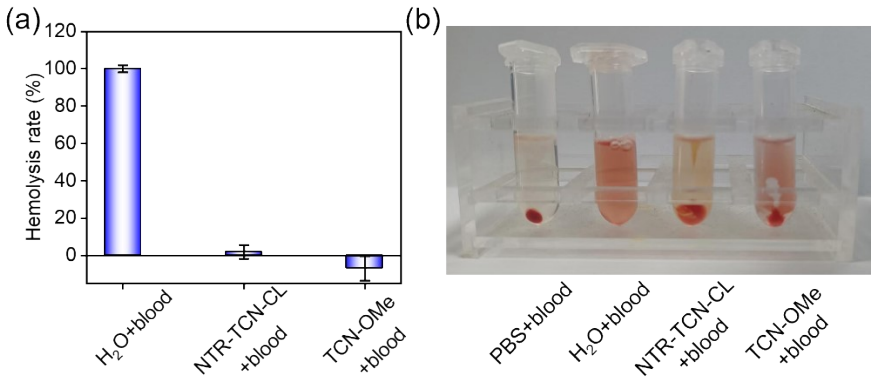

Fig. S32 (a) Hemolysis rate evaluation of **NTR-TCN-CL** (100 μM) and **TCN-OMe** (100 μM), (b) supernatant photograph of hemolysis test.

References

1 M. J. Frisch, G. W. Trucks, H. B. Schlegel, G. E. Scuseria, M. A. Robb, J. R. Cheeseman, G. Scalmani, V. Barone, G. A. Petersson, H. Nakatsuji, X. Li, M. Caricato, A. V. Marenich, J. Bloino, B. G. Janesko, R. Gomperts, B. Mennucci, H. P. Hratchian, J. V. Ortiz, A. F. Izmaylov, J. L. Sonnenberg, D. Williams-Young, F. Ding, F. Lipparini, F. Egidi, J. Goings, B. Peng, A. Petrone, T. Henderson, D. Ranasinghe, V. G. Zakrzewski, J. Gao, N. Rega, G. Zheng, W. Liang, M. Hada, M. Ehara, K. Toyota, R. Fukuda, J. Hasegawa, M. Ishida, T. Nakajima, Y. Honda, O. Kitao, H. Nakai, T. Vreven, K. Throssell, J. A. Montgomery, Jr., J. E. Peralta, F. Ogliaro, M. J. Bearpark, J. J. Heyd, E. N. Brothers, K. N. Kudin, V. N. Staroverov, T. A. Keith, R. Kobayashi, J. Normand, K. Raghavachari, A. P. Rendell, J. C. Burant, S. S. Iyengar, J. Tomasi, M. Cossi, J. M. Millam, M. Klene, C. Adamo, R. Cammi, J. W. Ochterski, R. L. Martin, K. Morokuma, O. Farkas, J. B. Foresman and D. J. Fox, *Gaussian 16, Rev. C.01. Gaussian, Inc., Wallingford, CT,* 2016.

2 K. Bruemmer, O. Green, T. Su, D. Shabat and C. Chang, *Angew. Chem. Int. Ed*., 2018, **57**, 7508 - 7512.

3 J. An, S. Tang, G. Hong, W. Chen, M. Chen, J. Song, Z. Li, X. Peng, F. Song and W. Zheng, *Nat. Commun.*, 2022, **13**, 2225.